CEA/SACLAY
DSM

SERVICE DE PHYSIQUE NUCLÉAIRE

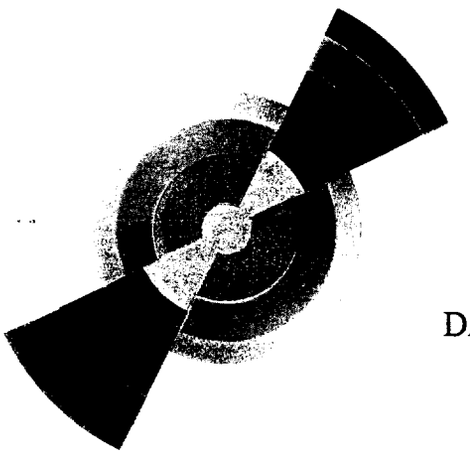

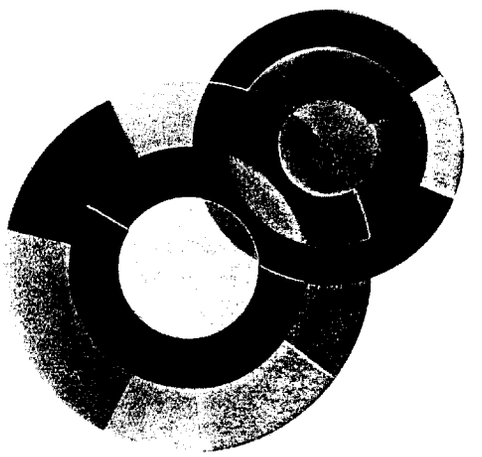

DAPNIA/SPhN-97-02 01/1997

Spin observables in pseudoscalar meson photoproduction

F. Tabakin and B. Saghaï

DAPNIA

Département d'**A**strophysique, de Physique des **P**articules, de Physique **N**ucléaire et de l'**I**nstrumentation **A**ssociée
CEA/Saclay F-91191 Gif-sur-Yvette Cédex

Couverture : Sylvie Cabrit et Marc Sauvage

Invited talk at « CEBAF/INT Workshop on
N* Physics »,
SEATTLE, sept. 8-13, 1996

SPIN OBSERVABLES IN PSEUDOSCALAR MESON PHOTOPRODUCTION

FRANK TABAKIN[*,a]
Department of Physics & Astronomy, University of Pittsburgh, Pittsburgh, PA 15260, U.S.A.

BIJAN SAGHAI
Service de Physique Nucléaire, CEA/DSM/DAPNIA, Centre d'Etudes de Saclay, F-91191 Gif-sur-Yvette, France

The energy evolution and angular structure of low energy pseudoscalar meson photoproduction spin observables are analyzed. Nodal trajectories, e.g. plots of angular nodes versus photon energy, and/or polynomial expansions are shown to be useful ways to identify effects due to underlying dynamics. Guidelines for the anticipated, or 'normal,' behavior of η photoproduction spin observables are generated based on several bold assumptions: (1) resonance dominance; (2) a feasible truncation of multipoles and (3) assuming negligible background effects. Observables that are particularly sensitive to missing nucleonic resonances predicted by quark-based approaches, are singled out.

1 Introduction

In a series of recent papers, [1,2,3,4] we have examined the question of how spin observables for meson photoproduction can be used to extract important dynamical features, such as resonances. Our motivation is to get a feeling for the general features of these spin observables, to classify them, and to be able to identify their "normal" behavior, in preparation for the plethora of data expected from TJNAF/CEBAF, ELSA, ESRF, LEGS and MAMI. It is well-known that spin observables can provide key dynamical information and that even their general features can provide important insights. For example, in proton-proton elastic scattering, the early cross-section measurements showed that, aside from the Coulomb peak, the cross-section is flat, at 32 MeV and even at 315 MeV, where P-waves were expected to contribute and to cause distinct angular variation. Various mechanisms were invented to suppress the P-waves, until the polarization of the final proton was found to be appreciable and to require P-waves. To explain the flatness of the cross-section, and the appreciable polarization, it was necessary to have significant P-waves for the polarization while the cross-section required small P-waves. The answer to this puzzle was that, in addition to a tensor force, a short-ranged spin-orbit interaction is needed, for which the P-waves average out, while they still contribute

[a] Presented talk.

to the polarization *via* S–P interference. The existence of a strong spin-orbit interaction of short range, sufficed for G. Breit [5] to predict the existence of a vector meson way before its discovery. (Vector meson exchange produces a strong $\vec{L} \cdot \vec{S}$ force.) That historical example, sets a challenge to us. Can we identify characteristics of the spin observables that can be used to identify basic dynamical characteristics? Our first step is to determine "normal" behavior of the spin observables.

2 Meson Photoproduction & Spin Observables

To understand the general characteristics of spin observables for pseudoscalar meson photoproduction, let us recall the definition of the 16 observables. In addition to the cross section, $\sigma(\theta)$, we have three single spin observables: the photon beam asymmetry (Σ), the target asymmetry (T), and the polarization (P) of the final baryon. There are also 12 double spin observables: four beam-target $\mathcal{BT}$, four beam-recoil $\mathcal{BR}$, and four target-recoil $\mathcal{TR}$. We are considering the meson (M) photoproduction reaction: $\vec{\gamma} + \vec{N} \rightarrow M + \vec{N}'$, where the photon beam can be polarized, the initial nucleon target is usually a proton, which can also be polarized, and the pseudoscalar mesons considered here are the π, η, or K. In the kaon case, the final (recoil) baryon is a Λ or a Σ, whose polarization can be measured *via* their decay (e.g. they are self-analyzing).

Four of the spin observables require circularly polarized photons; namely, two $\mathcal{BT}$ E, F plus two $\mathcal{BR}$ $C_{x'}, C_{z'}$ observables. Four double spin observables require linearly polarized photons; namely, two $\mathcal{BT}$ H, G plus two $\mathcal{BR}$ $O_{x'}, O_{z'}$ observables. In addition, the photon beam asymmetry, Σ, requires linearly polarized photons. For self-analyzing recoil baryons, the $\mathcal{BR}$ are feasible experiments; whereas, polarized targets are needed for the $\mathcal{BT}$ cases.

In the appendix, a bilinear helicity product classification of the 16 spin observables is briefly described, along with its use in determining the experiments needed to fully determine total amplitudes.

2.1 Legendre Classification

An additional way to classify the 16 observables is by their angular dependence. We refer to this classification scheme as "Legendre class." All observables depend on the scattering angle as:

$$\dot{\Omega}^\alpha = \Omega^\alpha \, \mathcal{I}(\theta) = \sum_L^{L_{max}} \bar{a}_L^\alpha P_L^m(\theta) = \sin^m \theta \, \mathcal{P}^\alpha(\theta) \equiv \sin^m \theta \sum_{L=0}^{L_{max}} a_L^\alpha \cos^L \theta. \quad (1)$$

where we define the "profile function" $\tilde{\Omega}^\alpha$ as the general observable Ω^α times the cross-section function $\mathcal{I}(\theta) \equiv (k/q)\ \sigma(\theta)$. Here $\alpha = 1 \cdots 16$ labels the 16 observables. An observable that has $m = 0, 1, or\ 2$ is of "Legendre class " $\mathcal{L}_m$. We recall [2] that the Legendre classes of the sixteen observables labeled by $\mathcal{L}_0$, $\mathcal{L}_{1a}$, $\mathcal{L}_{1b}$, and $\mathcal{L}_2$, are:
$\mathcal{L}_0(\mathcal{I}; E; C_{z'}; L_{x'})$, $\mathcal{L}_{1a}(P; H; C_{x'}; L_{x'})$, $\mathcal{L}_{1b}(T; F; O_{x'}; T_{z'})$, $\mathcal{L}_2(\Sigma; G; O_{z'}; T_{x'})$.
In the above list, the first entry in each class is the cross-section or a single polarization observable $(\mathcal{I}, P, T, \Sigma)$; the others are all double polarization observables, which appear ordered as Beam-Target (E, H, F, G), Beam-Recoil $(C_{z'}, C_{x'}, O_{x'}, O_{z'})$; with the last entry in each class being the Target-Recoil observables $(L_{z'}, L_{x'}, T_{z'}, T_{x'})$. From the $\sin^m \theta$ factor, we see that all but the $\mathcal{L}_0$ observables vanish at the 0° & 180° endpoints; the $\mathcal{L}_2$ class observables also have zero derivatives at the endpoints.

2.2 Nodal Trajectories

In the previous section, observables were classified by Legendre class with the general profile form $\tilde{\Omega}^\alpha = \sin^m \theta\ \mathcal{P}^\alpha$, where $\mathcal{P}^\alpha = a_0^\alpha + a_1^\alpha \cos\theta + a_2^\alpha \cos^2\theta + \cdots$ is a polynomial that can be truncated for sufficiently low final state momentum q. Photoproduction is an exothermic reaction and thus the underlying multipoles fall off as $(q \times range)^\ell$, where ℓ is the final meson-baryon orbital angular momentum and the "range" is typically the inverse mass of the lowest t-channel exchanged meson.

The polynomial coefficients a_L^α, which can be extracted from experiment, receive contributions from the electric and magnetic multipoles $E_\ell^\pm, M_\ell^\pm$, where the total angular momentum is $J = \ell \pm 1/2$. The N^* & Δ resonances, which have definite J & ℓ quantum numbers, feed into these multipoles and determine the strength and energy-dependence of the polynomial coefficients. Since each meson photoproduction reaction is characterized by a set of contributing resonances, the polynomial coefficients a_L^α, for each observable α, also have distinct behavior. We seek to identify characteristic signatures of underlying resonances, using the above polynomial structure.

One particularly important signature is the existence of nodes in an observable [b] and their associated energy dependence. Thus we consider the idea of nodal trajectories, [2] which is defined as a plot of the nodal angles θ_0, for which $\mathcal{P}(\theta_0) \equiv 0$, versus beam energy. Some sample nodal trajectory plots are shown in Fig. 1, where the 3D plots of an observable versus angle and energy are projected down to the $E-\theta$ plane. We have found nodal trajectories where: (1) a resonance drives the nodal angle to vary rapidly; (2) a bifurcation occurs,

[b] aside from the requisite behavior at the endpoints

Fig. 1. Typical energy and angular dependence of:(a) the $\mathcal{L}_0$ class $\mathcal{BT}$ double polarization observable E for kaon production, which demonstrates a bifurcation of nodes to satisfy the requirement that E have an even number of nodes. Double nodes appear because the $P_{13}(1720)$ resonance enhances the a_2 coefficient; (b) the $\mathcal{L}_2$ class photon polarization asymmetry Σ for kaon production, which displays a single node that moves rapidly from 180° toward 0° driven by a rapid variation of a_1 due to the $P_{13}(1720)$ resonance. A pair of nodes appears above 1.4 GeV, with increased a_2 due to $J = 5/2$, $t-$channel exchange for models without an explicit $J = 5/2$ resonance. The $SALY^6$ dynamical model is used for these illustrations.

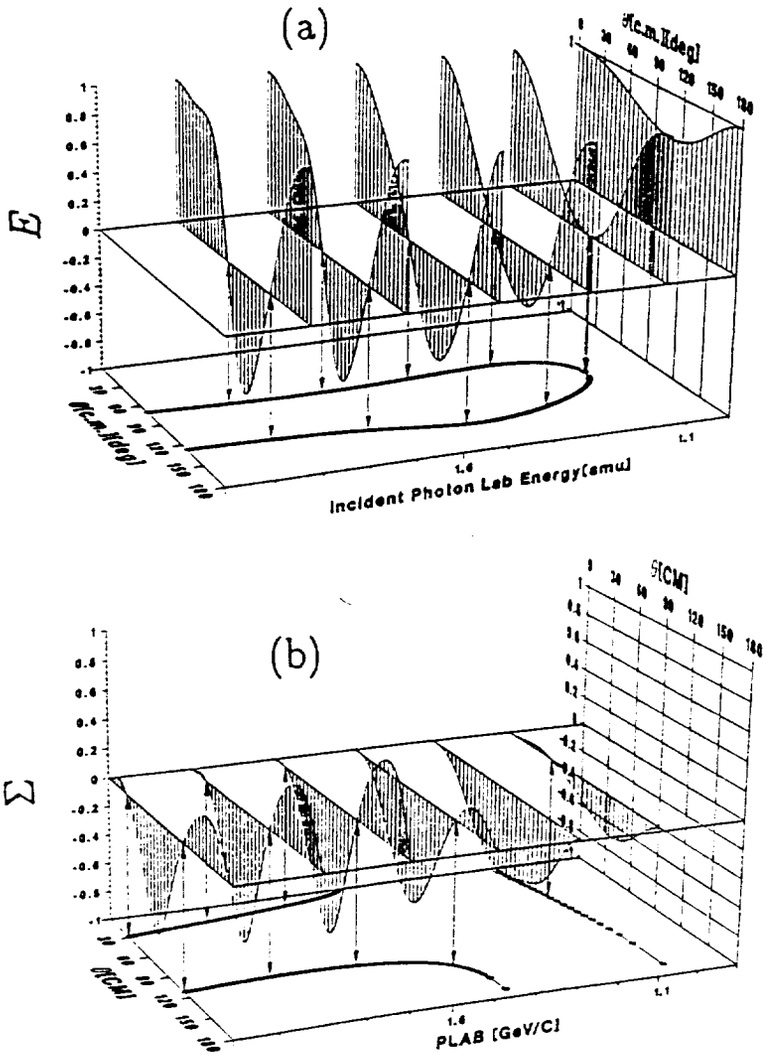

which means that nodal pairs appear and evolve–often in order to satisfy odd/even node theorems.[1,2] In addition, we have found cases where unexpected bifurcations occur at low energies driven by t–channel exchange mechanisms.[2]

Although the nodal trajectories can be used to identify particularly dramatic underlying dynamics, they are only part of the full information contained in the polynomial coefficients a_L^α.

3 Multipole Expansion for the Target Polarization

Let us consider a particular observable, the target asymmetry T, as an example of the electric and magnetic origins of the polynomial coefficients. The profile function $\tilde{T}(\theta)$ is of Legendre class $\mathcal{L}_{1b}$ and hence has the general form: $\tilde{T}(\theta) = \sin\theta \sum_{L=0}^{n} a_L \cos^L\theta$. The polynomial coefficients are given by the following imaginary parts of bilinear products of the electric, $E_\ell^\pm$, and magnetic, $M_\ell^\pm$, multipole amplitudes, where we are assuming that it is valid to truncate at $\ell \leq 3$ and $J \leq 5/2$:

$$
\begin{aligned}
a_0 &= Im\ \{3E_0^+[-E_1^+ + M_1^+ - E_3^- - M_3^-]^* - 3M_1^-[E_2^- + M_2^- + E_2^+ - M_2^+]^* \\
&\quad + E_1^+[-6\,E_2^- - 27/2\,E_2^+]^* + M_1^+[-6\,M_2^- + 15/2\,E_2^+ + 6\,M_2^+]^* + E_2^- \\
&\quad [6\,E_3^- - 15/2\,M_3^-]^* - 27/2\,M_2^-\,M_3^{-*} + 27/2\,E_2^+\,E_3^{-*} + 27/2 M_2^+\,M_3^{-*}\} \\
a_1 &= Im\ (3/2)\,\{2\,E_0^+[E_2^- + M_2^- - 4\,E_2^+ + 4\,M_2^+]^* + 2M_1^-[E_1^+ - M_1^+ + 4\,E_3^- \\
&\quad + 4\,M_3^-]^* - 3E_1^+[10\,E_3^- + M_3^-]^* + M_1^+[2\,E_3^- - 25\,M_3^-]^* + 8\,E_1^+\,M_1^{+*} \\
&\quad + E_2^-[25\,E_2^+ + 2\,M_2^+]^* + 3M_2^-[-E_2^+ + 10\,M_2^+]^* + 8\,E_2^-\,M_2^{-*} \\
&\quad - 18\,E_2^+\,M_2^{+*} + 36\,|E_3^-|^2 + 18\,|M_3^-|^2 - 18\,E_3^-\,M_3^{-*}\ \} \\
a_2 &= Im\ (3/2)\,\{10E_0^+[E_3^- + M_3^-]^* + 10M_1^-[E_2^+ - M_2^+]^* + 3E_1^+[4\,E_2^- - E_2^+ \\
&\quad + 10\,M_2^+]^* + M_1^+[12\,M_2^- - 25\,E_2^+ - 2\,M_2^+]^* + E_2^-[-2\,E_3^- + 25\,M_3^-]^* \\
&\quad + 3\,M_2^-[-10\,E_3^- - M_3^-]^* - 162\,E_2^+\,E_3^{-*} - 162\,M_2^+\,M_3^{-*}\ \} \\
a_3 &= Im\ (45/2)\,\{\,E_1^+[4\,E_3^- + M_3^-]^* + 3M_1^+\,M_3^{-*} - 3\,E_2^-\,E_2^{+*} \\
&\quad + M_2^-[E_2^+ - 4\,M_2^+]^* + 6\,E_2^+\,M_2^{+*} - 4\,|E_3^-|^2 + 2\,|M_3^-|^2 + 6\,E_3^-\,M_3^{-*}\ \} \\
a_4 &= Im\ (675/2)\,\{\,E_2^+\,E_3^{-*} + M_2^+\,M_3^{-*}\ \}.
\end{aligned}
\tag{2}
$$

Expressions for all other observables for $\ell \leq 2$ are available[3] and for $\ell \leq 3$ and $J \leq 5/2$ will be reported elsewhere[7].

It is worthwhile to analyze the structure of these expressions, where we are particularly motivated by the connection between: resonances, their associated multipoles and their influence on the polynomial coefficients, which finally affect the energy evolution and nodal structure of $\hat{T}$.

Under these assumptions, note that the a_0 term is driven by SP', PD, PD', ... interference, where we have invoked a simple notation that $S \equiv E_0^+$, while P' denotes the $P-$wave $J = 3/2$ (E_1^+, M_1^+) multipoles, P denotes the $P-$wave $J = 1/2$ (E_1^-, M_1^-) multipoles. Similarly, D' denotes the $D-$wave $J = 5/2$ (E_2^+, M_2^+) multipoles, D denotes the $D-$wave $J = 3/2$ (E_2^-, M_2^-) multipoles, and F stands for the $F-$wave $J = 5/2$ (E_3^-, M_3^-) multipoles. Using that abbreviated notation, the structures of a_0 to a_4 are described by:

$$a_0 \rightarrow \boxed{\text{S}}P' \oplus P\boxed{\text{D}} \oplus PD' \oplus P'\boxed{\text{D}} \oplus P'D' \oplus \boxed{\text{S}}F \oplus \boxed{\text{D}}F \oplus D'F.$$

$$a_1 \rightarrow P' \oplus \boxed{\text{D}} \oplus D' \oplus F \oplus \boxed{\text{S}}\boxed{\text{D}} \oplus \boxed{\text{S}}D' \oplus PP' \oplus \boxed{\text{D}}D' \oplus PF \oplus P'F,$$

$$a_2 \rightarrow PD' \ominus P'\boxed{\text{D}} \oplus P'D' \ominus \boxed{\text{S}}F \oplus \boxed{\text{D}}F \oplus D'F,$$

$$a_3 \rightarrow D' \ominus F \oplus \boxed{\text{D}}D' \oplus P'F, \; a_4 \rightarrow D'F,$$

where single letters denote terms like $D \rightarrow |E_2^-|^2$, $|M_2^-|^2$ *or* $E_2^- M_2^{-*}$ $D' \rightarrow |E_2^+|^2$, $|M_2^+|^2$ *or* $E_2^+ M_2^{+*}$ and $P' \rightarrow |E_1^+|^2$, $|M_1^+|^2$ *or* $E_1^+ M_1^{+*}$. Terms like SD continue to represent $S - D$ interferences. Note that the underlying tensor character of this observable yields the interesting, useful feature that $a_0, a_2 \cdots$ involve odd parity products, while $a_1, a_3 \cdots$ involve even parity products, which restricts how a multipole, and an associated resonance, can feed into the polynomial coefficients.

Another important feature of the above general analysis, is that for η meson photoproduction, it is reasonable to start from the experimental[8] and theoretical[9] results on the differential and total cross sections concluding that S & D amplitudes dominate *via* the $S_{11}(1535)$ and $D_{13}(1520)$ resonances. That makes the above 'boxed' terms most important. Thus, for a given scenario of a set of dominant resonances, it is often possible to make some general observations about the anticipated polynomial structure. Note that we are making several bold assumptions: (1) truncation of the amplitudes (which is valid only near threshold and perhaps near a dominant resonance); (2) that interference with the background can be neglected (at least qualitatively); and that (3) resonances dominate and characterize the observables. None of these assumptions are rigorously true and hence we are dealing with guidelines that can not replace a full dynamical treatment.

For an example of a simple limiting scenario, consider the case where the $S_{11}(1535)$ and $D_{13}(1520)$ dominate, Then, we have just S & D terms, e.g. just the $J = 1/2, E_0^+$, and $J = 3/2, E_2^-, M_2^-$, multipoles. Indeed, fits to the differential cross section for η meson photoproduction indicate that about 85% $S-$ and 15% $D-$wave suffice. In that case we see that $a_0 = a_2 = a_3 = a_4 = 0$, using our truncation. Then all the strength feeds into $a_1 = D \oplus SD$. The resultant $\sin\theta \times \cos\theta$ structure then indicates that a 90° node would exist in $\hat{T}$ for this particular resonance dominance and truncation scenario.

Another scenario is for a P, e.g. a P_{11} Roper and/or $P_{11}(1700)$, amplitude to play a small, but detectable, role in addition to the above S & D. In that case, $a_0 \rightarrow P\boxed{\text{D}}$ involves having the D_{13} magnify the P contribution to a_0, while $a_1 \rightarrow \boxed{\text{D}} \oplus \boxed{\text{S}}\boxed{\text{D}}$ remains dominant and a_2 to a_4 are still zero. In that case, T should have one node whose non-90° location is determined by the PD interference. Of course, the D and SD terms in a_1 could interfere destructively and/or a P resonance could occur to eliminate such a single node. Experiment will provide those insights.

If experiment indicates the need for a nonzero a_2 term, then under the SPD dominance and truncation scenario, we would be seeing a $a_2 \rightarrow P'D$ contribution, wherein the D magnifies a P' or P_{13} effect.

Recent data from Bonn [10] on the $\gamma\vec{p} \rightarrow \eta p$ provide angular distributions of the polarized target asymmetry T at six energies from roughly threshold up to 1 GeV. These are the first set of beneficial η photoproduction polarization data. Hence, we have applied our nodal structure approach to these data. The behavior of the polynomial coefficients show clearly that, in addition to the dominant $S_{11}(1535)$ and $D_{13}(1520)$, these data require contributions from P_{13} and D_{15} resonances and do not exclude the presence of the P_{11} resonance(s). We also explain why just the available cross-section data are not well suited for investigating (small) contributions from resonances other than the $S_{11}(1535)$ and $D_{13}(1520)$. Moreover, we confirm the presence of the P_{13} and D_{15} resonances in the dynamics by fitting the T-asymmetry data *via* a simple dynamical approach, where electric and magnetic multipole amplitudes are expressed in terms of various isospin-1/2 nucleonic resonances (described by "relativized" energy-dependent Breit-Wigner forms), plus a smooth background including S- and P- waves. That data [10] and our associated analysis [11] will be published soon.

The η photoproduction is especially interesting in searching [4,11] for the missing or undiscovered nucleonic resonances, which constitutes a crucial test of descriptions of baryon spectra. [12,13] The best observables to look for some of these resonances, as well as for manifestations of the Roper resonance, have been singled out. [4,11]

Finally, we have investigated the underlying dynamics in the pion and kaon photoproduction reactions,[2,4] our main findings are summarized below.

For pion photoproduction, our approach incorporates[4] some of the established facts; namely, that the reaction is dominated by the Δ_{33} resonance with non-negligible contributions from other spin 1/2 and 3/2 resonances. We also ascertained that the single and the double beam-target observables requiring a linearly polarized beam are the best observables for investigating the suspected contributions of spin 5/2 resonances.

We have also examined the strangeness photoproduction reaction, which has a rather complicated reaction mechanism. Based on our approach, we explain[4] the dynamical content of the phenomenological models.[14] Moreover, a clear manifestation[2] of the duality hypothesis in the strangeness sector has also been obtained.

4 Conclusions

We conclude that the angular structure of selected spin observables, especially for the η meson can be used to reveal amplitudes that might be resonances. Also the general structure of spin observables can be used to select the "best bet" observables for revealing hidden resonances. We hope that our general and qualitative discussion of spin observables and their angular dependence and energy evolution is a useful guide to both experiment and theory. We advocate that extraction of the polynomial coefficients is a useful guide and that the nodal trajectory analysis provides a particularly interesting way to track the appearance of resonance and other dynamical effects.

Acknowledgments

We are grateful to the organizers, as well as to INT-Seattle and TJNAF/CEBAF for their kind invitation to this stimulating workshop. We thank Mr. Wen-Tai Chiang for his help and Professors G. Anton and J. P. Didelez for having communicated their to us data prior to publication.

Appendix

Bilinear Helicity Product Form

In classifying spin observables, it is useful to describe the 16 profile functions $\hat{\Omega}^{\alpha}$ as combinations of bilinear products of helicity amplitudes. The mixture of these bilinear products, $H_i^* \; H_j \quad i,j = 1 \cdots 4$, needed to form these profile

functions are a complete set of hermitian 4×4 Γ^α matrices. We have:[15]

$$\tilde{\Omega}^\alpha = \frac{1}{2} \sum_{i,j} H_i^* \Gamma_{ij}^\alpha H_j \equiv \frac{1}{2} < H|\Gamma^\alpha|H > . \tag{3}$$

The Γ^α matrices are hermitian since the spin observables are real. This bilinear product form (BHP) allows us to map the algebra of the 16 observables and the 4 complex helicity amplitudes over to the well-known properties of hermitian versions of the standard 16 Γ^α matrices. The BHP for a general reaction with N amplitudes would map over to the N^2 complete set of $N \times N$ matrices, which could be view as a mapping of the N^2 observables over to an $N \times N$ Clifford algebra. For pseudoscalar photoproduction, $N = 4$ we have 4 helicity amplitudes.

Known properties of the 4×4 matrices can now be invoked as a short-cut to obtain relationships between observables. For example, consider the Fierz relationship (modified to apply to hermitian matrices)

$$\Gamma_{ij}^\alpha \, \Gamma_{st}^\beta = \sum_{\delta\eta} C_{\delta\eta}^{\alpha\beta} \, \Gamma_{it}^\delta \, \Gamma_{sj}^\eta \ , \tag{4}$$

where $C_{\delta\eta}^{\alpha\beta} \equiv \frac{1}{16}\mathrm{Tr}(\Gamma^\delta \Gamma^\alpha \Gamma^\eta \Gamma^\beta)$.

Applying the Fierz transformations to the BHP forms for spin observables, yields the following set of relations between observables:

$$\Omega^\alpha \, \Omega^\beta = \sum_{\delta\eta} C_{\delta\eta}^{\alpha\beta} \, \Omega^\delta \, \Omega^\eta \ , \tag{5}$$

where we have used $\tilde{\Omega}^\alpha \equiv \Omega^\alpha \mathcal{I}$ to reintroduce the observables Ω^α. Note that these relations hold true at all energies and all angles.

There are $16 \times 16 = 256$ choices for the pair α , β; however, due to symmetries and since many of the resulting equations are redundant, we can reduce the Fierz results to the 37 equations. These equations and evaluation of the coefficients $C_{\delta\eta}^{\alpha\beta}$, from trace rules are given in reference [15].

These 37 equations for the observables Ω^α $\alpha = 1 \cdots 16$ translate to the notation $(\sigma, \Sigma, -T, P)\,\mathcal{S}$; $(G, H, E, F)\,\mathcal{BT}$; $(O_x, -O_z, -C_x, -C_z)\,\mathcal{BR}$; $(-T_x, -T_z, L_x, L_z)\,\mathcal{TR}$, using the order $\alpha = (1, 4, 10, 12); (3, 5, 9, 11);$ $(14, 7, 16, 2); (6, 13, 8, 15)$.[16]

Assuming that all Type $\mathcal{S}$ observables $\Omega^{1,4,10,12}$ are measured, these 37 constraints are used in reference [16] to show that 8 carefully selected pseudoscalar meson photoproduction observables, rather than 9,[17] suffice to determine the 4 complex transversity total amplitudes free of discrete ambiguities.[18]

The above analysis maps the algebra of the 16 observables to an $SU(2) \times SU(2)$ or $SU(4)$ algebra. For the 12 complex vector meson photoproduction amplitudes, this BHP procedure generalizes to a $SU(4) \times SU(3)$ algebra, as demonstrated in reference[15], e.g. one has $\Gamma^\alpha \rightarrow \Gamma^\alpha \times \omega^\beta$, where ω^β, $\beta = 1 \cdots 9$, is a 3×3 basis.

References

[*] Research supported in part by the U. S. National Science Foundation.

1. C. G. Fasano, F. Tabakin and B. Saghai, Phys. Rev. C **46**, 2430 (1992).
2. B. Saghai and F. Tabakin, Phys. Rev. C **53**, 66 (1996).
3. P. Girard, B. Saghai and F. Tabakin, Saclay Report, DAPNIA-SPhN-96-01 (1996).
4. B. Saghai and F. Tabakin, "*Pseudoscalar meson photoproduction: from known to undiscovered resonances,*" Phys. Rev. C (1997), *under press.*
5. G. Breit, Phys. Rev. **120**, 287 (1960).
6. J.C. David, C. Fayard, G.H. Lamot, and B. Saghai, AIP Proceedings No 334 (1995), p.717.
7. B. Saghai and F. Tabakin, *in preparation.*
8. B. Krusche *et al.*, Phys. Rev. Lett. **74**, 3736 (1995); S.A. Dytman *et al.*, Phys. Rev. C **51**, 2710 (1995); J. W. Price *et al.*, *ibid.* C **51**, R2283 (1995).
9. M. Benmerrouche, Nimai C. Mukhopadhyay, and J.F. Zhang, Phys. Rev. D **51**, 3237 (1995); M. Bouché-Pillon, B. Saghai, and F. Tabakin, AIP Conference Proceedings No 339 (1995), p. 515.
10. G. Anton, A. Bock, and J. P. Didelez, *private communication* (1996).
11. B. Saghai, F. Tabakin, J. Ajaka, and P. Hoffmann-Rothe, *in preparation.*
12. R. Koniuk and N. Isgur, Phys. Rev. D **21**, 1868 (1980); S. Capstick and W. Roberts, *ibid* **47**, 1994 (1993); *ibid* D **49**, 4570 (1994).
13. F. Iachello, *these proceedings*; A. Leviatan *these proceedings.*
14. R. A. Adelseck and B. Saghai, Phys. Rev. C **42**, 108 (1990); R. Williams, C. Ji, and S. Cotanch, *ibid* C **46**, 1617 (1992); J.C. David, C. Fayard, G.H. Lamot, and B. Saghai, *ibid* C **53**, 2613 (1996).
15. M. Pichowsky, Ç. Şavkli and F. Tabakin, Nucl. Phys. **A370**, 311 (1994).
16. Wen-Tai Chiang and F. Tabakin, " *Completeness Rules for Spin Observables in Pseudoscalar Meson Photoproduction,*" preprint submitted for publication.
17. I. S. Barker, A. Donnachie, and J. K. Storrow, Nucl. Phys. **B95**, 347 (1975); and *these proceedings.*
18. G. Keaton and R. Workman, Phys. Rev. C **53**, 1434 (1996).